



ELSEVIER

Signal Processing 71 (1998) 187–201

**SIGNAL
PROCESSING**

Signature identification through the use of deformable structures

I. Pavlidis^{a,*}, N.P. Papanikolopoulos^b, R. Mavuduru^b

^a *Honeywell Technology Center, 3660 Technology Drive, MN65-2500, Minneapolis, MN 55418, USA*

^b *Department of Computer Science, University of Minnesota, 200 Union Street S.E., Minneapolis, MN 55455, USA*

Abstract

Automatic signature verification is a well-established and active research area with numerous applications. In contrast, automatic signature identification has been given little attention, although there is a vast array of potential applications that could use the signature as an identification tool. This paper presents a novel approach to the problem of signature identification. We introduce the use of the revolving active deformable model as a powerful way of capturing the unique characteristics of the overall structure of a signature. Experimental evidence as well as intuition support the idea that the overall structure of a signature uniquely determines the signature in the majority of cases. Our revolving active deformable model originates from the snakes introduced in computer vision by Kass et al., but its implementation has been tailored to the task at hand. This computer-generated model interacts with the virtual gravity field created by the image gradient. Ideally, the uniqueness of this interaction mirrors the uniqueness of the signature's overall structure. The proposed method obviates the use of a computationally expensive segmentation approach and is parallelizable. The experiments performed with a signature database show that the proposed method is promising. © 1998 Elsevier Science B.V. All rights reserved.

Zusammenfassung

Die automatische Verifikation einer Unterschrift ist weitgehend etabliert und ist ein aktives Forschungsgebiet mit zahlreichen Anwendungen. Im Gegensatz dazu wird der automatischen Identifikation von Unterschriften wenig Aufmerksamkeit entgegengebracht, obwohl ein weiter Bereich potentieller Anwendungen existiert, in dem die Unterschrift als Werkzeug zur Identifikation verwendet werden könnte. In diesem Artikel wird eine neue Annäherung an das Problem der Identifikation einer Unterschrift präsentiert. Wir führen die Verwendung des drehenden und aktiv verzerrenden Modells als mächtigen Weg ein, um die eindeutigen Charakteristika der gesamten Struktur einer Unterschrift herauszubilden. Experimentelle Beweise und Intuition unterstützen die Idee, daß die gesamte Struktur einer Unterschrift eindeutig die Unterschrift in der Mehrzahl aller Fälle determiniert. Unser drehendes und aktiv verzerrendes Modell entspringt den Schlangen, die von Kass und anderen in der Computervision eingeführt wurden, aber die Implementation wurde auf die vorliegende Aufgabe zugeschnitten. Dieses mittels Computer generierte Modell arbeitet interaktiv mit dem virtuellen Schwerfeld zusammen, daß von dem Bildgradienten erstellt wird. Idealerweise spiegelt die Eindeutigkeit dieser Interaktion die Eindeutigkeit der gesamten Struktur einer Unterschrift wieder. Die vorgeschlagene Methode beugt der Verwendung eines rechenaufwendigen Segmentierungsansatzes vor und ist parallelisiert. Die Experimente mit einer Unterschriftsdatenbank zeigen, daß die vorgeschlagene Methode vielversprechend ist. © 1998 Elsevier Science B.V. All rights reserved.

* Corresponding author. Tel.: +1 612 9517338; fax: +1 612 9517438; e-mail: pavlidis@htc.honeywell.com.

Résumé

La vérification automatique de signatures est un domaine bien établi, où les recherches sont actives, et qui possède de nombreuses applications. Par contre, l'identification automatique de signature a reçu peu d'attention, malgré le fait qu'il y ait un large domaine d'applications potentielles qui pourraient utiliser la signature comme un outil d'identification. Cet article présente une nouvelle approche du problème de l'identification de signatures. Nous introduisons l'utilisation de modèles déformables actifs pivotants comme un moyen puissant de capturer la caractéristique unique de la structure globale d'une signature. Des évidences expérimentales de même que l'intuition supportent l'idée que la structure globale d'une signature la détermine de façon unique dans la majorité des cas. Notre modèle déformable actif pivotant repose sur les serpents (snakes) introduits en vision par ordinateur par Kass et al., mais son implémentation a été adaptée à la tâche à réaliser. Ce modèle général par ordinateur interagit avec le champ de gravité virtuel créé par l'image gradient. Idéalement, l'unicité de cette interaction reflète l'unité de la structure globale de la signature. La méthode proposée supprime l'utilisation d'approches de segmentation chères en temps de calcul, et est de plus parallélisable. Les expériences faites avec une base de données de signatures montrent que la méthode proposée est prometteuse. © 1998 Elsevier Science B.V. All rights reserved.

Keywords: Signature identification; Revolving active deformable model; Virtual gravity field; Virtual springs; Synchronized string matcher

1. Introduction

The recognition of characters, numerals and graphics by computers, and the automatic verification of signatures has been an active research topic for more than 20 years [1–3,9–11,15–18]. Now-a-days, we have reached the point where both graphics and text can be recognized in machine-generated documents and some research and commercial signature verification prototypes have demonstrated their feasibility. However, recognition of highly cursive script still remains a partially solved problem [9] and automatic signature identification has been given little attention so far.

The automation of signature verification and identification has been justified in a number of papers for financial as well as security reasons

[3,9,16]. Signature identification searches for the identity of a given signature through a signature database (Fig. 1). Signature verification verifies whether a given signature belongs to a specified individual (Fig. 2). Apparently, the signature identification problem is more complex than the signature verification problem and little research effort has been focused on this area.

It is customary to distinguish *on-line* from *off-line* signature identification and verification systems. In an on-line system the user has to sign on an electronic tablet which typically gives a signal $z(t) = [x(t), y(t)]^T$ (i.e., image coordinates as a function of time). This system enables dynamic information such as stroke sequence, acceleration, and in some cases pressure to be captured in real time. On the other hand, in an off-line system the user does

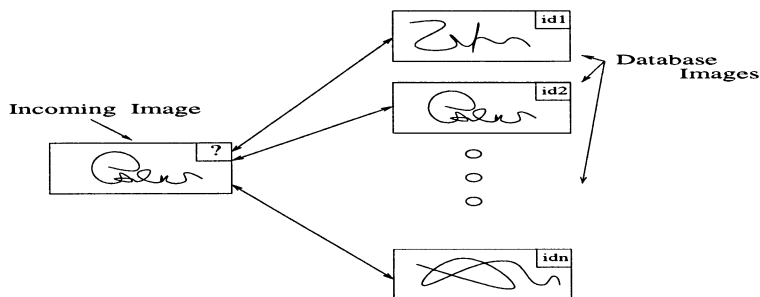


Fig. 1. Signature identification.

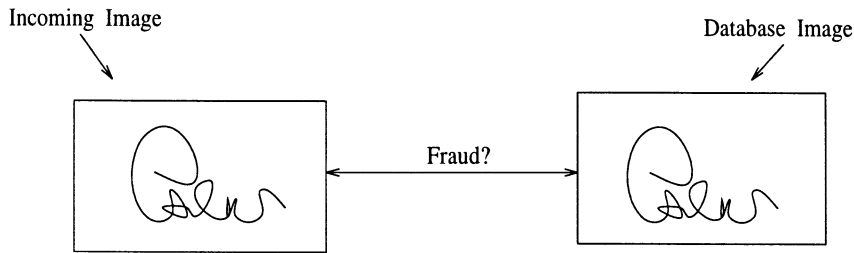


Fig. 2. Signature verification.

not use a tablet but instead he/she signs on a paper and his/her signature is captured via a camera or a scanner (static image). Obviously, the dynamic information that can be so easily extracted in the on-line method, it is very difficult or impossible to be recovered in the off-line method. Dynamic information is of special value to verification systems since the forger might be able to copy the overall shape of the owner's signature but it would be almost impossible to copy the timing and the rhythm with which it is written.

The handwritten signature is considered to be among the best means for an automated personal identification system. It can be produced nearly anywhere and unlike passwords or identity cards cannot be forgotten or lost [3]. It is also advantageous in terms of psychological factors when compared with other biometric methods. Signature identification appears not to bother people, perhaps because signing is a common everyday activity. Quite to the contrary, eye recognition, for example – both retina scanning, which requires close contact with the recognition device, and iris scanning, which can be done from a more comfortable distance – disconcerts some people because of an inherent protectiveness about their eyes.

An intelligent signature identification system, in which the user does not have to go through the awkward procedure of laying an identity claim by punching an ID number (verification) would be of great value. Instead, the system should be capable of arriving at a foolproof identification decision (identification and verification) based solely upon the signature of the user. Such a system is the ultimate goal of the line of research we are pursuing. We consider the problem of foolproof signa-

ture identification as a two-stage process. In the first stage, signature identification through static image analysis should be achieved. The second stage should verify that indeed the signature has been written by the user whose identity has been recovered in the first stage and not by a skillful impostor. In this second stage the use of on-line information would be essential (hybrid system). In the identification stage, the unique characteristics of the signature's overall structure are captured first. Then, if the system cannot arrive at a definite conclusion, it should resort to a more detailed – and more time-consuming – investigation of the signature's structure. Experimental evidence [13] as well as intuition support the idea that the overall structure of a signature uniquely determines the signature in the majority of cases. Only for a relatively small percentage of problematic signatures, the system would need to resort to the detailed structure analysis module.

In this paper we address the problem of identifying signatures by capturing the unique characteristics of their overall structure. As will be explained in subsequent sections, by introducing the use of the revolving active deformable model, we manage to capture the signature's overall shape in such a way that at the same time it conveys information about the signature's internal structure. Thus, while we maintain the simplicity, the intuitiveness and the speed of the global methods, we achieve at the same time descriptive details comparable to that obtained by localized methods, without resorting to a computationally expensive and heavily heuristic segmentation approach. Interestingly, speed can be further increased by exploiting the parallelization potential of the algorithm. The organization

of the paper is as follows. Section 2 presents some previous work conducted in the area. Section 3 outlines the proposed system. Sections 4–7 describe in detail the various modules of our system. In Section 8 the experimental results are presented. Finally, in Section 9 the paper is summarized and conclusions are drawn.

2. Previous work

Traditionally, the bulk of the static techniques can be classified into one of the following three categories [9]:

- *Global approach.* In the global approach the features are extracted from every pixel that lies within a rectangle circumscribing the signature. Typical global techniques include transformations [11] and image gradient analysis [17]. Although the global methods are easy and insensitive to noise, they deteriorate when significant distortion and style variations are present and satisfactory position alignment cannot be achieved.
- *Statistical approach.* The statistical features are derived from the statistical distribution of the signature's pixels. The statistical approach is more tolerant than the global methods to distortion and style variations since it incorporates a certain amount of topological and dynamic information [1,2].
- *Geometrical and topological approach.* The geometrical and topological features describe the characteristic geometry and topology of a signature. Geometrical and topological features can

tolerate a high degree of distortion and style variations, and they can even tolerate up to a certain degree translational and rotational variations [9].

3. Outline of the system

The geometrical and topological approach gives the most detailed description of the signature image. Geometrical and topological feature extraction in conventional methods is primarily based upon segmentation techniques. Segmentation usually leads to a heavily heuristic approach and places a considerable burden on the computational process. Our approach departs totally from this mode of tracing signatures off-line. Instead of segmenting the signature, we rather follow a *holistic* approach.

We address the problem of capturing the overall structure of a signature by using a technique that is well established in the area of active vision for tracking objects [5] but has never been tried before in the field of signature identification and verification. We introduce the use of a computer-generated *revolving active deformable model* as a powerful means of capturing the overall structure of a signature in considerable detail. Our revolving active deformable model is similar, but not exactly the same with the snakes introduced by Kass et al. [8]

More specifically, the proposed method consists of four modules (Fig. 3):

1. *Preprocessing.* Preprocessing includes a thresholding operation to clear up the image and an orientation normalization procedure that facilitates the identification process.

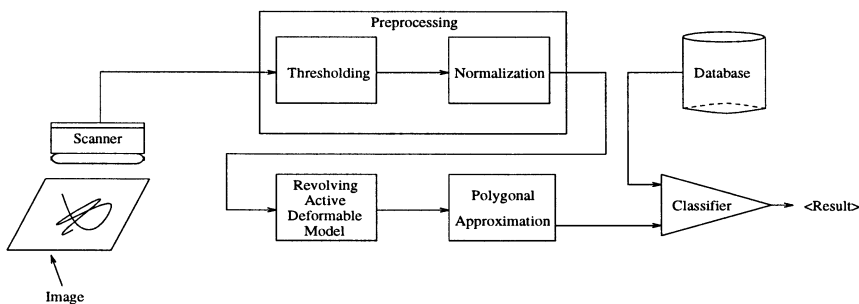


Fig. 3. Block diagram of the signature identification system.

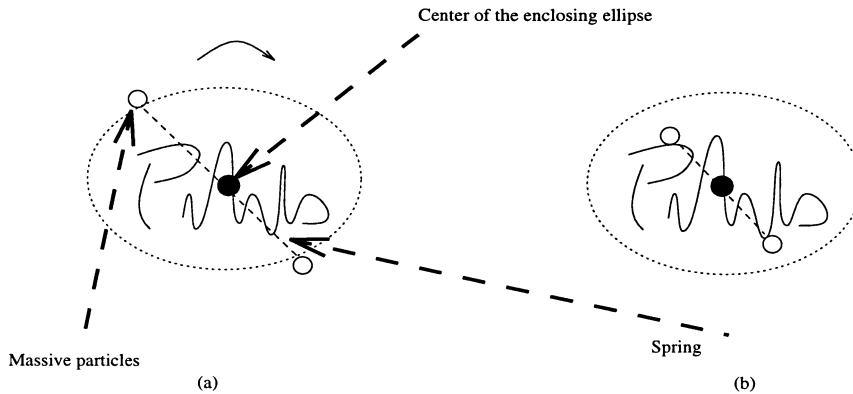


Fig. 4. Instance of a revolving active deformable model: (a) initial position; (b) final position.

2. *Revolving active deformable model.* This is the main part of the whole procedure. Two-particle active deformable models are applied to the signature (Fig. 4). The particles are connected through an elastic spring that goes through the center of an enclosing ellipse. The particles lie initially on the enclosing ellipse 180° apart. Each pair of particles gets attracted to the signature edges, locally, under the combined influence of the virtual spring and of a virtual gravity field generated by the image gradient. The pairs of particles are applied in a revolving fashion at equally spaced angular intervals and at high resolution (5° apart). Each pair of particles reaches finally a stable condition leaving a trace on the signature's boundary. At the end, the sequence of all these traces gives an abstraction of the signature's structure.
3. *Polygonal approximation.* The key in signature identification is to distinguish between the signature's habitual parts and those that vary in almost every sample of the signature. While the application of the revolving active deformable model at high resolution is essential in focusing on certain important characteristics, like deep, narrow valleys, at certain signature parts it gathers excessive information (e.g., like small fluctuations of almost straight lines, which might be of some value for verification purposes, but are rather harmful for identification purposes). A polygonal approximation algorithm is applied at this time, to smooth such detrimental detail

out of the set of points gathered from the previous module.

4. *Classification.* A string feature vector is composed out of the internal angles of the polygonal shape reported by the previous module. Then, classification based upon a novel string matching algorithm (the Synchronized String Matcher (SSM)), developed specifically for the task at hand is performed and a unique match between the signature image and a prototype signature stored in the signature database is established. In the case of failure to come up with a clear-cut match, the system classifies the case as inconclusive.

4. Preprocessing

4.1. Thresholding

It is very important for the main processing module of an identification system to be applied to a noise-free image. We actually need a binary signature image where the signature body will clearly stand out in a perfectly clean background. This is especially true for the case of active deformable models, because salt and pepper noise can totally alter the virtual gravity field of the image. We also need the thresholded signature image to represent the sampled signature as faithfully as possible, since the best identification technique would be useless if applied to a heavily distorted image.

The thresholding technique chosen for that purpose is a method devised by [12]. It involves a non-parametric and unsupervised method of threshold selection. An optimal threshold is selected, in order to maximize the separability of the resultant classes in gray levels. The algorithm utilizes only the zeroth- and the first-order cumulative moments of the gray-level histogram and is very fast.

4.2. Normalization

The normalization process involves only an orientation normalization and not a size normalization. The classifier module later classifies according to features that are size invariant. More specifically, a signature is oriented in such a way that its elongation axis is horizontal. The alignment of the elongation axis with the horizontal axis (*x-axis*) is achieved through the use of second-order spatial moments [6].

Utilizing only second-order moments for orienting a 2-D shape leaves us with a *two-way ambiguity*. The elongation axis has been properly aligned to the horizontal axis of the coordinate system, but it is not known if the oriented shape should be rotated by 180° or not (that is, which part should face east and which should face west). To resolve this matter we could resort to the determination of the most distant point from the centroid or alternatively to higher-order moments [7]. Either of these methods is going to fail for some signatures. The reason is that some signatures have an almost symmetrical shape, that favors slightly sometimes the northern, sometimes the southern part, some other times the western or the eastern part, depending on the ‘mood’ of the signer. These kinds of signatures render any further orientation processing useless. The problem has been overcome by processing both the aligned image yielded by the above orientation algorithm and its flipped (rotated by 180°) version for each prototype signature image. The results of this processing are kept into two separate fields, one for the aligned reference image and one for its flipped version, and linked with the node of the corresponding prototype signature database entry. A test signature image is oriented by using the second-order spatial moments only, it is pro-

cessed, and the result of processing is matched against both fields of every reference signature database entry.

5. Revolving active deformable model

An active deformable model is a mesh of artificial massive particles connected to each other by artificial elastic springs. Each particle interacts with the signature image through attracting forces created by high values in the image-gradient map. The movement of the active deformable model on the image plane is governed by the laws of classical mechanics. Our active deformable models are modeled after the active deformable models used by Couvignou et al. [5] for visually tracking moving objects with two notable differences. First, our active deformable models are not used in tracking moving objects but rather in capturing the overall structure of static signature images. Second, we do not arrange the mesh of particles in a rectangular fashion around the signature, but we rather apply pairs of particles in succession, along the enclosing ellipse of the signature, at equally spaced intervals and in a revolving fashion. This mode of active deformable model application (revolving active deformable model) not only yielded dramatic performance gains but entailed the method to be potentially fully parallelizable.

In more detail, the enclosing ellipse of the signature is defined as the ellipse whose foci are the middle points of the left and right edges of the bounding rectangle. The particles are connected through an elastic spring that goes through the center of the ellipse. The particles lie initially on the enclosing ellipse 180° apart. We chose the starting positions of the particles to be on the enclosing ellipse, because it gives us a nice parametric model to achieve half a revolution around the signature, and in addition, it circumscribes the signature more closely than any other simple closed curve, facilitating a strong interaction with the signature’s gravitational field. The pairs of particles are applied in a revolving fashion at equally spaced angular intervals (5° apart). Each pair of particles gets attracted to the signature edges, locally, under the combined influence of the spring forces and of a virtual



Fig. 5. Snapshot of a revolving active deformable model in action – during the initial phase.

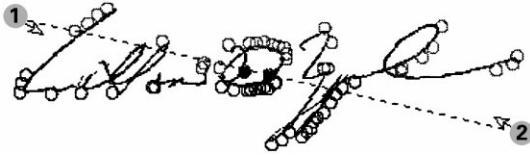


Fig. 6. Snapshot of a revolving active deformable model in action – during the final phase.

gravity field. The pair finally reaches a stable condition, represented pictorially by small circular traces on the signature's boundary (see Figs. 5 and 6).

The particles are moving in the image plane, and the motion of each i th particle obeys the classical dynamic equation

$$m_i \ddot{\mathbf{r}}_i = \mathbf{F}_i^{\text{ext}} + \sum_{j=1}^n \mathbf{F}_{ij}^{\text{int}}, \quad (1)$$

where m_i is the mass of the i th particle, $\mathbf{r}_i = (x_i, y_i)^T$ is the position vector of the i th particle in the image plane, $\mathbf{F}_i^{\text{ext}}$ is the *external force*, exerted by sources external to the system of particles, and $\mathbf{F}_{ij}^{\text{int}}$ is the *internal force* exerted on the i th particle by the j th particle. External forces are created by the image gradient magnitude of the signature's pixels. Internal forces are spring forces and their main function is to bring the pair of particles from its initial position on the enclosing ellipse where the gravitational field is non-existent or weak, closer to the signature image, where the gravitational field becomes stronger and can define the trajectories of the particles. In our case, the sum of internal forces is trivialized to $\mathbf{F}_{12}^{\text{int}}$ since our active deformable model consists of only two particles.

5.1. Internal forces

Internal forces are created by virtual massless linear springs with viscous friction. Thus, the par-

ticles are connected together through a mesh of *damped linear springs*. In our case, since we use only pairs of particles, only a single linear spring is necessary. The internal force $\mathbf{F}_{ij}^{\text{int}}$ is given by the formula

$$\mathbf{F}_{ij}^{\text{int}} = \kappa_{ij}(\mathbf{r}_{ij} - \mathbf{r}_{ij}^0) \frac{\mathbf{r}_{ij}}{r_{ij}} - l_{ij} \dot{\mathbf{r}}_{ij} \frac{\mathbf{r}_{ij}}{r_{ij}}, \quad (2)$$

where $\mathbf{r}_{ij} = \mathbf{r}_i - \mathbf{r}_j$ is the relative position vector of particle j with respect to particle i , and r_{ij} is the distance between particle i and particle j . The term κ_{ij} is the linear stiffness, \mathbf{r}_{ij}^0 is the viscous friction coefficient, and l_{ij} is the length at rest of the linear damped spring that connects the particles i and j together. We have determined experimentally that best system performance is achieved for the following parameter values: $\kappa_{ij} = 0.6$, $r_{ij}^0 = 0.8$ and $l_{ij} = 1.4$.

5.2. External forces

The external force $\mathbf{F}_i^{\text{ext}}$ on the i th particle m_i is created by the image; it is expressed as the sum of two forces,

$$\mathbf{F}_i^{\text{ext}} = \mathbf{F}_i^{\text{grav}} + \mathbf{F}_i^{\text{damp}}. \quad (3)$$

The image gravitational force $\mathbf{F}_i^{\text{grav}}$ attracts the particle m_i to the image contours. Like in [5], we opted to implement these contour attracting forces with a gravitational force field proportional to $\mathbf{r}/(r^2 + b^2)$ (where b is a positive scalar constant) instead of the classical Newtonian form \mathbf{r}/r^3 . This formulation has been motivated by a computationally efficient implementation, as well as the need to obtain finite values for the gravity force at $r = 0$, which is not the case with the Newtonian gravity field.

Let $I(s)$ denote the intensity at pixel s whose image coordinates are (x, y) . The image gradient is computed inside a square window $W(i)$ centered at particle i . The best compromise between computation time and steady attraction was achieved by a 41×41 -pixel window. All pixels s in $W(i)$ are assigned a virtual mass $M(s)$ whose value is the magnitude of the image gradient:

$$M(s) = \|\nabla I(s)\|. \quad (4)$$

The elementary virtual mass $M(s)$ attracts the mass m_i of the particle i to the pixel s with a force whose magnitude is a function of the distance r_{si} . The gravitational force acting on the mass m_i of the particle i is expressed as

$$F_i^{\text{grav}} = -\frac{1}{\bar{M}_i} G_0 \sum_{s \in W(i)} M(s) \frac{r_{si}}{r_{si}^2 + b^2}, \quad (5)$$

where G_0 is the gravity constant, b is a positive scalar constant, and \bar{M}_i is the average virtual mass in the window $W(i)$, which means

$$\bar{M}_i = \frac{1}{W_i^2} \sum_{s \in W(i)} M(s), \quad (6)$$

where $W_i = 41$.

The damping force F_i^{damp} smooths the motion of the system in the image plane, as though the whole set of particles was bathed in a viscous liquid, so that

$$F_i^{\text{damp}} = -V\dot{r}_i, \quad (7)$$

where V is the viscous friction coefficient. This smoothing effect is necessary during the initial phase of attraction, from the time the active deformable model leaves the enclosing ellipse until the time the gravitational field becomes strong enough to outweigh all the other factors. The reason is that since the forces (external and internal) are updated in the current system at the frequency of 10 Hz, unconstrained spring forces (with no smoothing factor present) might prove faster-acting than the update frequency and manage to retract the particles too far away from the position anticipated, before the gravity field becomes strong enough to dominate the particle's trajectory. We have also determined experimentally that the following parameter values produce the best results: $G_0 = 0.6$, $b = 10.0$ and $V = 4.3$.

The window $W(i)$ centered at the particle i within which the virtual gravity field that affects the trajectory of particle i is computed, it reaches over time image areas well beyond the outermost edges of the signature. Thus, the internal structure of the signature plays a role too in the definition of the particle trajectories. It is obvious now why the traces left by the revolving active deformable model do not merely constitute a polygonal ap-

proximation to the overall shape of the signature but in addition, they mirror the overall structure of the signature.

5.3. Gaps in the signature image

The problem encountered with the revolving active deformable model is that of significant gaps found in some signature images, typically, gaps between the first and last name of the signer. In those cases, the particles, under the dominant influence of the spring forces are likely to cross each other and one or both get stabilized somewhere in the boundary of the semi-image which is complementary to their original target, due to the 'hole' in the virtual gravity field. Thus, the particle from the lower part of the signature image may end up in the upper part and vice versa (see Figs. 7 and 8). This is obviously detrimental to the cause of following the signature's outline. It is also detrimental to



Fig. 7. Behavior of the revolving active deformable model in signature gaps – the particles due to the gap are not stabilized in their image part and under the influence of the spring force tend to cross to the other image part (e.g., particle 2 moves towards the upper part of the image); the inter-particle distance is decreasing.



Fig. 8. Behavior of the revolving active deformable model in signature gaps – the particles have crossed to the complementary image parts where they will eventually get stabilized (e.g., particle 2 is now in the upper image part and continues to move); the inter-particle distance is increasing again signaling the detection mechanism to ignore the traces of the particular pair of particles.

the cause of mirroring the signature's structure since the behavior of the particles is almost exclusively defined by the spring forces and not by the image gravitational forces.

A scheme has been developed for the system to detect the occurrence of gap particle behavior and exclude the corresponding traces from further consideration. More specifically, the pattern of behavior of the pair of particles in the gaps is that the particles first approach each other, and thus the distance r_{ij} between them tends to 0, and then they start getting away from each other as they move towards the complementary parts of the image, thus having the inter-particle distance r_{ij} increased again. This pattern of behavior is captured by a detection mechanism and the traces of these particles are left out of consideration.

6. Polygonal approximation

The points gathered from the application of the revolving active deformable model define already a polygonal approximation to the overall shape of the signature. The question is why do we apply a specific polygonal approximation algorithm at this time to further reduce the number of points we carry, and do not apply the revolving active deformable model at lower resolution (say 30°) in order to achieve the same objective. The answer is that the application of the revolving active deformable model at high resolution is essential in focusing on certain discriminating features of high value, like deep narrow valleys, that would be skipped altogether if the revolving active deformable model is applied at a lower resolution. At the same time, this high-resolution application of the revolving active deformable model gives a rather jagged effect in small, almost straight lines, that renders matching of almost similar polygonal shapes impossible (see Figs. 9–11).

Fig. 9. shows the result of the application of the revolving active deformable model at high resolution (5°) with no subsequent polygonal approximation phase. One can see the jagged effect which is especially pronounced along nearly straight lines, like the end of the signature in the particular figure. In fact, the very small line segments along the



Fig. 9. Revolving active deformable model applied at 5° resolution with no subsequent polygonal approximation phase.



Fig. 10. Revolving active deformable model applied at 5° resolution with subsequent polygonal approximation phase.

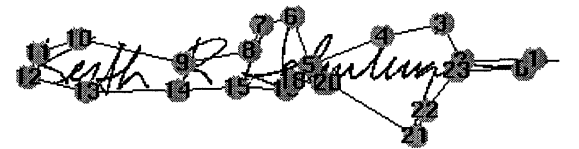


Fig. 11. Revolving active deformable model applied at 30° resolution with no subsequent polygonal approximation phase.

straight parts of the signature are imperceptible in the figure because they are covered by the numbered vertices of the polygonal shape. Fig. 10 shows the final result after an application of the revolving active deformable model of equal resolution as that in Fig. 9 (5°), but with a subsequent polygonal approximation phase. One can witness the elimination of the jagged effect, while at the same time the polygonal shape remains almost the same. In Fig. 11 the revolving active deformable model has been applied at a lower resolution (30°) achieving a reduction in points comparable with Fig. 10. It should be noted how crucial discriminating features like the two consecutive valleys between vertices 8 and 12 in Fig. 10 have disappeared in Fig. 11.

A simple splitting algorithm which has been widely used [14] has been chosen in order to carry out the polygonal approximation phase. The tolerance E_{\max} has been tuned to 5 pixels. Experimental

runs with our current signature database, confirmed that $E_{\max} = 5$ yields the best results (i.e., it smooths out the jagged effect without compromising the accuracy of the polygonal representation).

7. Classification

7.1. Similarity measure

The points produced by the polygonal approximation algorithm represent an approximation of the signature's overall shape. At the same time, these points, as was explained in Section 5, convey information about the internal structure of the signature. All this information in order to be useful for matching purposes needs to be transformed into another more appropriate form. The internal angles of the polygonal shape have been chosen as its defining feature. The computation of each internal angle is achieved through the use of the dot and cross products of its sides. More specifically, starting from the initial vertex 0 of a polygon with n vertices, as we walk counterclockwise around the shape, at each vertex k ($k = 0, \dots, n - 1$), we compute first the unit vectors starting from the vertex and lying along its polygonal sides and subsequently we compute the dot and cross products of these vectors. The dot product yields an angle ω_k which happens to be the internal angle θ_k when the cross product indicates a clockwise turn or in other words a convex curve (see Fig. 12). In case the cross product indicates a counterclockwise turn or differently speaking a concave curve (Fig. 12), then the internal angle is $\theta_k = 360^\circ - \omega_k$.

Angles are coded into one of 18 possible symbols A, \dots, R , corresponding to 20° increments; i.e. $A: 0^\circ < \theta \leq 20^\circ$; $B: 20^\circ \leq \theta < 40^\circ$; ... $R: 340^\circ < \theta \leq 360^\circ$. The strings formed in this way constitute the feature vectors of the signature images. Suppose that two polygonal fits, D and E , of two signature images, are coded into strings following the above scheme and let us denote those strings as $d_1 d_2 \dots d_n$ and $e_1 e_2 \dots e_m$, respectively. There are two kinds of matches that may occur between the symbols of the two strings: a *full match* and a *half match*. A full match occurs if $d_k = e_j$, where k and j may be different in the general case. A half match occurs if

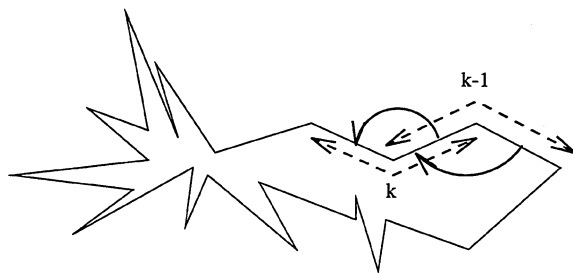


Fig. 12. Computation model for the internal angles. At vertex $k - 1$, the cross product of its directional edges (dashed arrows) indicates a clockwise turn (convex curve), while at vertex k , it indicates a counterclockwise turn (concave curve).

$d_k - 1 = e_j$ or $d_k + 1 = e_j$, where again k and j might be different in the general case too. Let H represent the number of credit points accrued from the matches between the two strings according to the following scheme: a full match gathers two credit points and a half match gathers one credit point. Half matches account, basically, for the high variability factor found in some signatures of the same individual. A perfect match would accrue $2 * |D| = 2 * |E|$ credit points, where $|\text{arg}|$ is the length (number of symbols) in the string representation of the argument. Thus, a non-perfect match differs

$$J = 2 * \max(|D|, |E|) - H \quad (8)$$

credit points from a perfect match. Of course, $J = 0$ if and only if $|D|$ and $|E|$ are identical. The similarity measure between D and E according to which classification is done is the ratio

$$Q = \frac{H}{J} = \frac{H}{2 * \max(|D|, |E|) - H} \quad (9)$$

Hence, Q is infinite for a perfect match and zero when none of the symbols in D and E match ($H = 0$ in this case). Due to implementation restrictions, in perfect match cases Q is set to the maximum integer available on the machine. Because matching is done symbol by symbol, the starting point on each boundary is important in terms of reducing the amount of computation. This is the reason that an orientation normalization stage preceded this module. The starting point is always the left trace left from the very first application of the revolving active deformable model.

The system is trained by using one sample signature of every individual we consider as a user of the system. The feature vectors of both the aligned and the flipped version of each such reference signature are established and stored in the system database along with the corresponding id. Then, the system tries to match the feature vector of each test signature with one of the feature vectors of the reference signatures using the similarity measure Q . The largest value of Q signifies the best match. The value of Q should be above a certain threshold in order for the match to be successful.

7.2. String matching

The usual string matching strategy followed in pattern recognition problems is a sequential one. Starting from the starting symbol, symbols are compared one by one until we run out of symbols for the shortest string. This technique does not work very well in signature identification and perhaps is not quite suitable for other pattern recognition problems of similar difficulty. The reason is that due to the variability factor typically present in the signatures of the same individual, the corresponding polygonal approximations may differ locally at some areas, although they maintain pretty much the same shape overall.

For a matching process that proceeds in a sequential manner once the first significant difference in the outline between the test signature and the corresponding reference signature is encountered, the process is derailed and is unable to catch subsequent parts of great similarity between the two polygonal shapes. This situation is exemplified in Figs. 13 and 14. At vertex 4, a sequential matching algorithm will fail and it will cause a derailment that will affect all the subsequent matches. Thus, the comparison between the test image (Fig. 14) and the reference image (Fig. 13) will accrue very few or no credits after vertex 3. Alternatively, the process can continue by advancing the vertex pointer in the test image of Fig. 14 to vertex 6 and the vertex pointer in the reference image of Fig. 13 to vertex 5. From there we can obtain successful matches until the end of the polygonal chain. A novel algorithm, the Synchronized String Match-

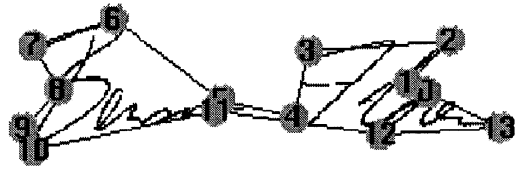


Fig. 13. Reference signature image.

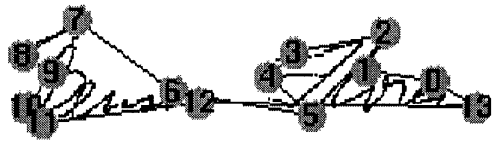


Fig. 14. Test signature image corresponding to the reference signature image of Fig. 13.

er (SSM), inspired from error recovery techniques in compiler design, but tailored to the task at hand, has been developed to cope with the particular problem.

SSM Description. Essentially, the SSM algorithm tries to resynchronize the matching process between the reference signature string and the test signature string, after each derailment, always within a prespecified distance (number of lookahead symbols) L . In order to apply the algorithm we need to know which string has the minimum length between the test string and the reference string. Let $minlen$ be the length of the shorter string and $maxlen$ the length of the longer string. In addition, $imin$ and $imax$ are two indices pointing initially at the first symbols of the corresponding strings. In case the strings have equal lengths, $minlen$ is the length of the reference string and $imin$ traces the reference string. Let also U be the number of consecutive unsuccessful matches since the last successful match took place. It is also important to note that H is the number of credit points accrued from the symbol matches of two strings. Then, the SSM algorithm in pseudocode form could be expressed as follows:

```

SSM(L)
1  U ← 0
2  H ← 0
3  while (imin < minlen) and (imax < maxlen)
4     case: Successful match

```

```

5       $imin \leftarrow imin + 1$ 
6       $imax \leftarrow imax + 1$ 
7       $U \leftarrow 0$ 
8      if full match
9          then  $H \leftarrow H + 2$ 
10         else  $H \leftarrow H + 1$ 
11 case: Unsuccessful match
12 if ( $U < L$ )
13     then if ( $(imax - imin) > L$ ) or
        ( $imax = (maxlen - 1)$ )
14         then  $imax \leftarrow imax - U$ 
15              $imin \leftarrow imin + 1$ 
16              $U \leftarrow 0$ 
17         else  $imax \leftarrow imax + 1$ 
18              $U \leftarrow U + 1$ 
19     else  $imin \leftarrow imin + 1$ 
20          $imax \leftarrow imax - L$ 
21          $U \leftarrow 0$ 
22         if ( $imin - imax > L$ )
23             then  $imax \leftarrow imax + 1$ 
24 return  $H$ 

```

The pseudocode notation we use conforms to the notation introduced by Cormen et al. [4]. One could observe that the lookahead search conducted after each derailment never extends further than L symbols (L has been set to 3 in our system). In addition, the $imin$ and $imax$ pointers are always kept not further apart than L symbols. This L -symbol barrier ensures that the matching derailment is due to some variation in the signatures of the same individual and not due to something more serious, like a signature shape that is only remotely similar in some parts with our test signature. It also ensures that the matching parts share the same orientation, that is, a part in the left upper part of one signature does not match with a similar part in the bottom middle part of another signature. Table 1 shows a trace of the SSM algorithm when it is applied to the signatures of Figs. 13 and 14. The $imin$ and $imax$ indices in Table 1 take the number values of the polygonal vertices that correspond to the string symbols the two indices are pointing at. The situation is clarified in Fig. 15 where the status of the computation is depicted in detail during the second step of the trace listed in Table 1.

Table 1

Trace left by the SSM when applied to the signatures of Figs. 13 and 14

Step	$imin$	$imax$	Match	Number of credit points, H
1	0	0	No match	0
2	0	1	No match	0
3	0	2	No match	0
4	0	3	No match	0
5	1	0	No match	0
6	1	1	Full match	0
7	2	2	Half match	2
8	3	3	No match	3
9	3	4	No match	3
10	3	5	No match	3
11	3	6	No match	3
12	4	3	No match	3
13	4	4	No match	3
14	4	5	No match	3
15	4	6	No match	3
16	5	3	No match	3
17	5	4	No match	3
18	5	5	No match	3
19	5	6	Full match	3
20	6	7	Half match	5
21	7	8	Full match	6
22	8	9	Half match	8
23	9	10	Half match	9
24	10	11	Half match	10
25	11	12	Full match	11
26	12	13	No match	13
27	13	13	Full match	13

8. Experimental results

The user population of the system is currently 60 individuals. The system has been trained with one sample signature from each individual user. The system has been tested with 180 test signatures, three from each user. The test signatures have been collected at different days and times and no restrictions have been applied. The individuals participating in the experiment were asked to sign on a plain piece of paper using a pen or a pencil. Plain paper and not textured paper, like the one used in checks, was used, to imitate the conditions under which the final foolproof identification system is intended to operate. For example, the final form of the system could be a platform similar to current hand-held communicators, like the Newton[®] of Apple, where

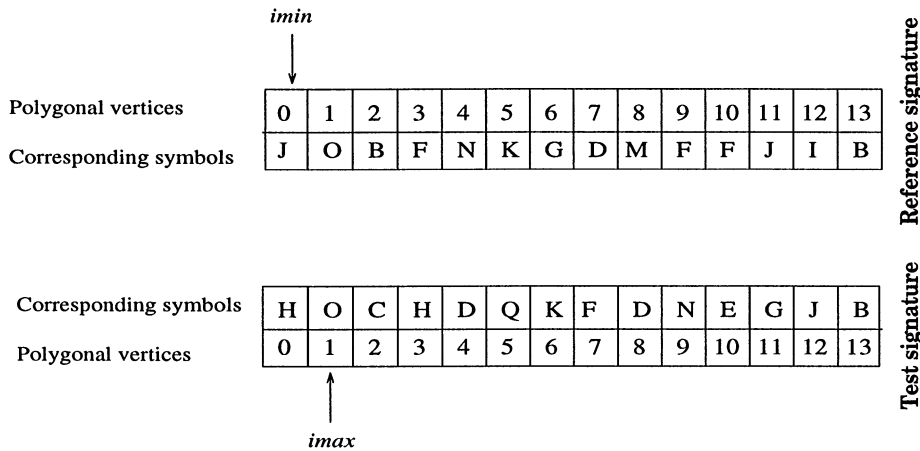


Fig. 15. Computation status during step 2 of the SSM trace shown in Table 1. Because there was no match in step 1, *imax* advances to the first lookahead symbol, while *imin* does not move.

both image data and dynamic information will be captured simultaneously. The test subjects were graduate and undergraduate students and various professionals. Out of 180 test signatures, 142 have been correctly identified which amounts to 78.89% success rate, 33 test cases have been signaled as inconclusive (18.33%), and for the remaining 5 signatures (2.78%) the system gave false recognition. The test results are summarized in Table 2. Fig. 16 shows sample test signatures (columns b and c) that were successfully matched with the corresponding reference signatures (column a). Only signature 1c was classified as inconclusive since it features a middle initial that is absent in the corresponding reference signature. Fig. 17 shows the sensitivity of the final identification result with respect to the angular resolution of the snake.

The system uses two kinds of thresholds. One threshold has been set up to disallow signatures of individuals who are not registered users of the system to weakly match some random reference signature, thus allowing intrusion in to the system. Experimentation with the current system led us in characterizing all matches that yield similarity measures $Q < 0.9$ as weak matches and therefore rejecting the corresponding test signatures as signatures belonging to invalid users. The other threshold has been set up in order to direct very close – and thus, questionable – matches to the perspective detailed structure analysis system for further

Table 2
Test results

Correct	Inconclusive	False
142 or 78.89%	33 or 18.33%	5 or 2.78%

investigation. Thus, if the difference of the similarity measures between the best match and the second best match, $\Delta Q < 0.2$, the current system classifies the match as inconclusive.

The main reason for the failures (which is the true detrimental element of the current system) is that the signatures of certain individuals exhibit great variability and as a result their structure differs noticeably in certain areas. The system, although in general copes quite well with those problematic signatures, there is a certain kind of signature variability that it cannot address successfully. This regards strokes that vary in length from trial to trial and sometimes cover significant part of the signature outline while other times do not (see Figs. 18 and 19). Strokes of this type sometimes ‘hide away’ a significant portion of the internal structure of the signature while they reveal it some other times, resulting into substantially different feature vectors. Because the matching is done part by part by the SSM mechanism, if the part of the signature image that is not affected by the on–off behavior of the stroke (invariant) is similar with some part of

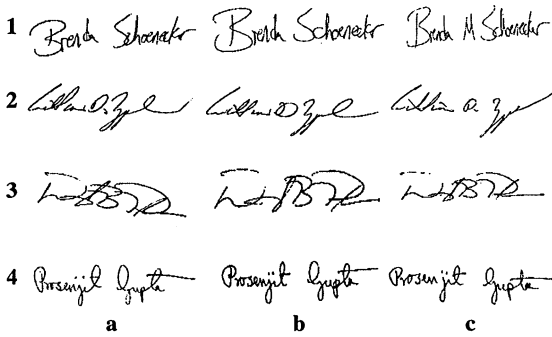


Fig. 16. Signatures successfully identified by the system. Column a shows the reference signatures while columns b and c the actual test signatures. Signature 1c is an exception since it was classified as an inconclusive case.

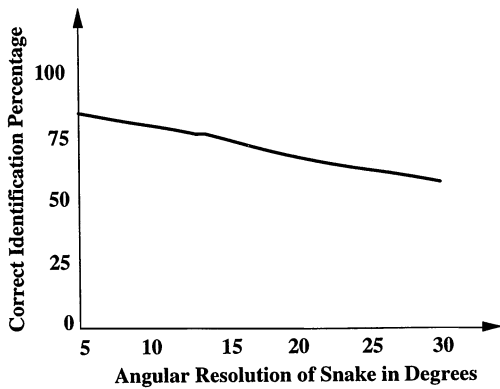


Fig. 17. Sensitivity of the identification result with respect to the angular resolution of the snake

another irrelevant reference signature image, it may lead to false identification.

The only way to establish a successful match and avoid a false identification in cases like the above, is to have the revolving active deformable model approximate the parts that remain similar in great detail, so that no valuable points get lost. The revolving active deformable model, as it stands, fails to do so sometimes because the spring forces proved too restrictive. Thus, some features of great discriminating value like deep narrow valleys may be represented in the polygonal approximation as shallow valleys, because the spring forces prohibit the particles of falling all the way down to the bottom of the valley. Under-represented discrimi-

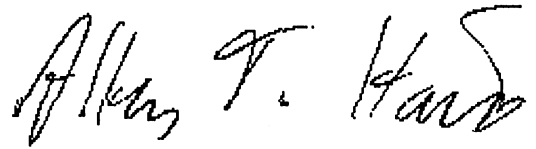


Fig. 18. Reference signature image.



Fig. 19. Test signature image differing noticeably from the corresponding reference signature image of Fig. 18.

nating features in a pattern that is already quite different from its corresponding reference pattern may give advantage to roughly similar reference patterns and lead to false recognition. A way out of this problem would be to have the spring forces out of the way once the particles are well within the range of the image gravity field. In addition, keeping more than one signature samples from each user in the reference database and building the reference vector of each user entry by applying an averaging process upon all the relevant reference samples would increase the robustness of the system.

It takes the system on average 17.1 s to arrive at an identification decision on the current implementation platform (IRIS Indigo™ R4000). Almost the entire time is spent during the application of the revolving active deformable model phase. It is expected that the above time will be drastically reduced once the system migrates to parallel hardware and the revolving active deformable model algorithm is properly parallelized. The differential equations that describe the motion of all the 36 pairs of particles (the number that corresponds to 5° angular resolution) could be solved in principle in parallel.

9. Conclusion

In this paper, we addressed the question of whether elastic structures similar to snakes

introduced by Kass et al. [8] can be of some value as a first stage classifier in the area of signature identification and verification. The most important contribution of this work is the introduction of the revolving active deformable model as a powerful mean for capturing the signature's overall structure. The experiments confirmed that signatures are uniquely determined by their overall structure in the great majority of cases. Identification rates are satisfactory for a first stage classifier, and the system responds reasonably fast. Speed, however, will increase dramatically once we exploit the parallelization potential of the model.

Future research efforts will focus on diminishing the false identification rate. This is the most important hurdle before we move on to the verification part of our perspective system, since the verification process for these false identified cases will be meaningless. We need to transfer as much as possible out of the false percentage to the inconclusive percentage. Then, the perspective detailed structure analysis system will be able to resolve the ambiguity. In that respect, an increase to the approximating power of the revolving active deformable model by utilizing the spring forces only as an initialization device will help considerably.

Acknowledgements

We thank the students of the Cs5561-day and Cs5116-extension classes during the academic year 1993–94 as well as the faculty members and the staff of the Computer Science Department at the University of Minnesota, who kindly provided us with their signatures. This work has been supported by the Graduate School of the University of Minnesota through contracts #1546-521-5998, by the National Science Foundation through contracts #IRI-9410003 and #IRI-9502245, and by the McKnight Land-Grant Professorship Program of the University of Minnesota.

References

[1] M. Ammar, Y. Yoshida, T. Fukumura, A new effective approach for off-line verification of signatures by using pressure features, in: Proc. 8th Internat. Conf. on Pattern Recognition, 1986, pp. 566–569.

- [2] M. Ammar, Y. Yoshida, T. Fukumura, Description of signature images and its application to their classification, in: Proc. 9th Internat. Conf. on Pattern Recognition, 1988, pp. 23–26.
- [3] J.J. Brault, R. Plamondon, A complexity measure of handwritten curves: modeling of dynamic signature forgery, *IEEE Trans. Systems Man Cybernet.* 23 (4) (1993) 400–413.
- [4] T.H. Cormen, C.E. Leiserson, R.L. Rivest, *Introduction to Algorithms*, The MIT Press, Cambridge, MA, 1989.
- [5] P.A. Couvignou, N.P. Papanikolopoulos, P.K. Khosla, Hand-eye robotic visual servoing around moving objects using active deformable models, in: Proc. Internat. Conf. on Intelligent Robots and Systems, 1992, pp. 1855–1862.
- [6] R.M. Haralick, L.G. Shapiro, *Computer and Robot Vision*, Addison-Wesley, Reading, MA, 1992, Vol. 1, Chapter 3, pp. 59–75.
- [7] B.K.P. Horn, *Robot Vision*, Chapter 3, The MIT Press, Cambridge, MA, 1986, pp. 63.
- [8] B. Kass, A. Witkin, D. Terzopoulos, Snakes: Active contour models, *Internat. J. Comput. Vision* 1 (4) (1987) 321–331.
- [9] S. Lee, J.C. Pan, Off-line tracing and representation of signatures, *IEEE Trans. Systems Man Cybernet.* 22 (4) (1992) 755–771.
- [10] S. Mori, C.Y. Suen, K. Yamamoto, Historical review of OCR research and development, in: Proc. IEEE 80 (7) (1992) 1029–1058.
- [11] W.F. Nemcek, W.C. Lin, Experimental investigation of automatic signature verification, *IEEE Trans. Systems Man Cybernet.* 4 (1) (1974) 121–126.
- [12] N. Otsu, A threshold selection method from gray-level histograms, *IEEE Trans. Systems Man Cybernet.* 9 (1) (1979) 62–66.
- [13] I. Pavlidis, R. Mavuduru, N. Papanikolopoulos, Off-line recognition of signatures using revolving active deformable models, in: Proc. IEEE Internat. Conf. on Systems Man, Cybernetics 1994, pp. 771–776.
- [14] T. Pavlidis, *Structural Pattern Recognition*, Springer, Berlin, 1977, pp. 175–179.
- [15] R.I. Phelps, A holistic approach to signature verification, in: Proc. 6th Internat. Conf. on Pattern Recognition, 1982, pp. 1187.
- [16] R. Plamondon, G. Lorette, Automatic signature verification and writer identification – the state of the art, *Pattern Recognition* 22 (2) (1989) 107–131.
- [17] R. Sabourin, R. Plamondon, Preprocessing of handwritten signatures from image gradient analysis, in: Proc. 8th Internat. Conf. on Pattern Recognition, 1986, pp. 576–579.
- [18] C.Y. Suen, M. Berthod, S. Mori, Automatic recognition of handprinted characters – The state of the art, *Proc. IEEE* 68 (4) (1980) 469–487.